Collection efficiency of optical photons generated from microwave excitations of a Bose-Einstein condensate

Árpád Kurkó,[1,*] Peter Domokos,[1] David Petrosyan [2] and András Vukics [1,†]

[1]*Wigner Research Centre for Physics, P.O. Box 49, H-1525 Budapest, Hungary*
[2]*Institute of Electronic Structure and Laser, Foundation for Research and Technology–Hellas, GR-70013 Heraklion, Crete, Greece*

Stimulated Raman scattering on Λ atoms is a promising tool for generating optical photons from a microwave excitation in the ground-state hyperfine manifold. We consider an atomic Bose-Einstein condensate coupled to a microwave field that scatters photons into the guided modes of a nearby optical fiber. Due to momentum transfer to the condensate, stimulated photon scattering can occur outside of the phase-matched direction, which can be used to separate the converted photons from the strong Raman readout pulse. Conversely, in the phase-matched direction, superradiant scattering due to bosonic enhancement leads to an increased collection efficiency in the guided modes of the fiber, for which we determine optimal conditions.

I. INTRODUCTION

A quantum network consists of a set of quantum processing and storage nodes distributed at different locations and connected by optical fibers that transmit quantum information via photons [1–3]. Various platforms with experimentally verified relevant quantum capabilities have been proposed for the implementation of the nodes. These include nuclear magnetic resonance systems [4], single trapped ions [5], neutral atoms in optical lattices [6], single atoms in optical cavities [7], quantum dots [8,9], color centers in crystals [10], and, perhaps the most promising, superconducting circuits [11,12]. The latter platform operates in the microwave regime, and quantum-coherent microwave-to-optical converters [13] will play a key role in the realization of a quantum network with superconducting-circuit nodes [14]. This is, however, a daunting task since for the microwave-to-optical conversion at a single-photon level, strong and coherent coupling is needed between quantum degrees of freedom differing by many orders of magnitude in energy. The most promising recent experiments employed hybrid systems to realize transducers, demonstrating remarkable achievements, including bidirectional operation [15], coherent coupling [16,17], and efficient conversion [18,19]. Moreover, there has also been recent progress in systems outside atomic, molecular and optical physics realizing microwave-to-optical transducers by means of radiation pressure [20,21].

Neutral alkali or alkaline-earth atoms have strong optical transitions and also microwave resonances between hyperfine sublevels and thereby provide a natural platform for realizing a quantum transducer at a single-photon level [22]. In many situations of interest, such atoms can be modeled as three-level systems with a Λ configuration of levels. A single

microwave photon [23,24] can be converted into a spin-wave excitation of the atomic hyperfine sublevels, which, in turn, can be transferred to a single optical photon in a stimulated Raman process that is inherently reversible [25,26]. In Refs. [27,28], Rydberg transitions of the atoms were proposed as an alternative route to achieve strong dipole coupling to a microwave field.

In the Λ configuration, a hyperfine transition of a single atom does not have sufficient interaction strength with a microwave photon to make a practically useful transducer. The natural mitigation is to use large ensembles of atoms [22,28]. In this paper we study the generation of an optical photon from a spin-wave-like microwave excitation of a degenerate quantum gas [a Bose-Einstein condensate (BEC)] with large coherence length compared to the optical wavelength. Trapping an atomic BEC in the vicinity of a superconducting waveguide resonator and coupling the hyperfine atomic states to the microwave resonator field [29,30] has already been achieved [31].

Already in the early days of Bose-Einstein condensation experiments, two essential features of light scattering on a BEC were noted: superradiance due to bosonic enhancement and the possibility for the light to excite density waves that extend coherently over the whole atomic sample [32,33]. We note that phenomena of the same physical origin were more recently found to lead to dynamical phase transitions and exotic phases when the BEC interacts with a resonator field [34–41] instead of the free-space electromagnetic field, whereas the quantum state of the BEC can be imprinted on that of the light [42–44].

Here we consider a BEC in a stimulated Raman process. Since the generated optical photons are envisaged for applications in quantum communication, we consider how efficiently such photons can be coupled into guided Gaussian modes focused on an optical fiber by a paraxial optical array [22]. We focus on the spatial profile of the generated radiation, which is encoded not only in the spatial

_____
*curko.arpad@wigner.hu
†Corresponding author: vukics.andras@wigner.hu

dependence of the readout Gaussian mode but also in the overlap integrals between the condensate state at different stages. As the core of our work consists of the analysis of the geometrical factors, we formulated our results independently of the explicit form of the time-dependent internal dynamics, concentrating on the incoupling efficiency and not on the efficiency of a microwave-optical transduction. Although the internal dynamics is formally similar to the ones encountered in stimulated Raman adiabatic passage (STIRAP) or electro-magnetically induced transparency (EIT), a full treatment of the coupling of the internal dynamics and the atomic motional degrees of freedom is beyond the scope of this work: here we restrict ourselves to a perturbative treatment. Our results will thus be relative to that of a single-atom scheme, extracting the consequences of having many atoms with the spatial extension of a BEC cloud.

Since the light scattering can create excitations in the BEC that are associated with atomic momentum, the condensate participates in the momentum balance of the stimulated Raman process. In particular, the BEC can take away almost arbitrary momentum from the photonic part of the process without significantly altering its energetics. This is because the dispersion relation of the BEC excitations is extremely flat on the momentum scale relevant to optical photons due to the large atomic mass. The photon scattering can then occur in the directions other than the phase-matched one determined by the readout light. This side scattering has an intensity proportional to the number of atoms in the condensate. For the forward-scattering case, with the photon emitted in the phase-matched direction, however, we find a superradiant be-havior, with the condensate returning to the ground state and the scattered intensity being proportional to the square of the atom number in the BEC. Exact momentum conservation can be violated because the BEC state is not an atomic momentum eigenstate, and a Gaussian beam is not a momentum eigen-state for the light. We identify situations where, due to these weak violations of the momentum conservation, the direction of the maximum of even the forward-scattered intensity devi-ates from the direction of the readout pulse.

This paper is organized as follows. In Sec. II, we in-troduce the scheme mixing the microwave field, the optical readout pulse, the generated optical photon, and the BEC excitation. We use a second-quantized description in which the equations of motion can be written straightforwardly in the single-excitation subspace. In Sec. III, we introduce our theory for emission of the generated optical photon into parax-ial guided (Gaussian) modes. Since for a given direction such modes still form a broadband one-dimensional continuum around the frequency of the emitted radiation, the radiated intensity can be written in the Born-Markov approximation, similar to free-space spontaneous emission. We distinguish two cases: (i) side scattering with the BEC left with a single free-particle excitation and (ii) forward scattering with the BEC returning to its initial state. In Sec. IV, we present our numerical results and discuss the findings.

II. THE FOUR-WAVE MIXING SCHEME

We consider a Bose-Einstein condensate of atoms with the ground state $|g\rangle$, a hyperfine state in the ground-state manifold
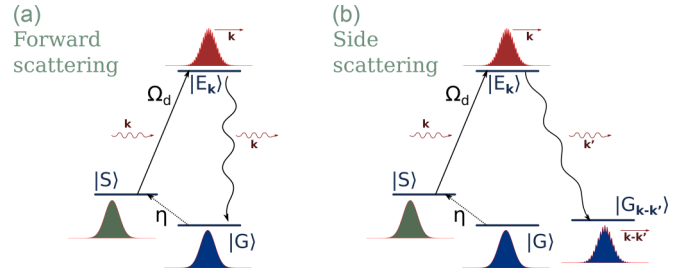

FIG. 1. Level scheme depicting the many-body states available to the system starting from $|G\rangle \equiv |0, 0, 0\rangle$. The other states are defined as $|S\rangle \equiv |0, 1, 0\rangle$, $|E_\mathbf{k}\rangle \equiv |0, 0, 1_\mathbf{k}\rangle$, and $|G_\mathbf{k}\rangle \equiv |1_\mathbf{k}, 0, 0\rangle$. Black lines with arrows show the transitions induced by the interaction with the microwave cavity, the drive, and the free elec-tromagnetic fields.

$|s\rangle$, and an excited state $|e\rangle$ in the Λ configuration of levels (see Fig. 1). Transition $|g\rangle \rightarrow |s\rangle$ is coupled to a microwave resonator mode $\hat{c}$ of frequency ω_c with coupling strength η. The hyperfine magnetic substates $|g\rangle$ and $|s\rangle$ are coupled by electric dipole transitions to the excited state $|e\rangle$. An ex-ternal laser of frequency ω_d resonantly drives the transition $|s\rangle \rightarrow |e\rangle$ with Rabi frequency Ω_d. The transition $|g\rangle \rightarrow |e\rangle$ is coupled to the free-space modes of the electromagnetic field $\hat{a}_{\mathbf{k},\lambda}$ of frequency ω_k with strength $g_{k,\lambda}$. Setting $\hbar = 1$, the single-atom Hamiltonian is

$$H = \frac{\mathbf{P}^2}{2M} + U(\mathbf{r})(|g\rangle\langle g| + |s\rangle\langle s|) + \omega_{gs}|s\rangle\langle s| + \omega_{ge}|e\rangle\langle e|$$
$$+ \left(\eta\,\hat{c}\,e^{-i\omega_c t}|s\rangle\langle g| + \Omega_d\,e^{-i\omega_d t}\,e^{i\mathbf{k}_d\mathbf{r}}|e\rangle\langle s| \right.$$
$$\left. + \sum_{\mathbf{k},\lambda} g_{k,\lambda}(\mathbf{r})\,\hat{a}_{\mathbf{k},\lambda}\,e^{-i\omega_k t}|e\rangle\langle g| + \mathrm{H.c.} \right), \qquad (1)$$

where $\mathbf{P}^2/2M$ is the kinetic energy the atom can acquire from the momentum transfer from the electromagnetic radiation and $U(\mathbf{r})$ is an optical dipole trapping potential for the atom in states $|g\rangle$ and $|s\rangle$, while the atom in the excited state is assumed to be free. The diagonal terms of the Hamiltonian proportional to ω_{gs} and ω_{ge} can be eliminated in a rotating frame, leading to

$$H = \frac{\mathbf{P}^2}{2M} + U(\mathbf{r})(|g\rangle\langle g| + |s\rangle\langle s|)$$
$$+ \left(\eta\,\hat{c}\,|s\rangle\langle g| + \Omega_d\,e^{i\mathbf{k}_d\mathbf{r}}|e\rangle\langle s| \right.$$
$$\left. + \sum_{\mathbf{k},\lambda} g_{k,\lambda}(\mathbf{r})\,\hat{a}_{\mathbf{k},\lambda}\,e^{-i(\omega_k - \omega_{ge})t}|e\rangle\langle g| + \mathrm{H.c.} \right), \quad (2)$$

where we assumed resonant interactions $\omega_c = \omega_{gs}$ and $\omega_d = \omega_{se}$.

The second-quantized Hamiltonian can be derived from Eq. (2) as $\hat{H} = \int dV\,\hat{\Psi}^\dagger(\mathbf{r})H\,\hat{\Psi}(\mathbf{r})$ using the field-operator ansatz (written in spinor notation that formally yields a ket in the Hilbert space of internal atomic states; see, e.g.,

Ref. [45])

$$\hat{\Psi}(\mathbf{r}) = \sqrt{N}\,|g\rangle\,\phi_{\text{BEC}}(\mathbf{r}) + \sum_{\mathbf{p}\neq 0}|g\rangle\,\phi_{\mathbf{p}}(\mathbf{r})\,\hat{b}_{g\,\mathbf{p}}$$

$$+ \sum_{\mathbf{p}}|s\rangle\,\phi_{\mathbf{p}}(\mathbf{r})\,\hat{b}_{s\,\mathbf{p}} + \sum_{\mathbf{p}}|e\rangle\,\phi_{\mathbf{p}}(\mathbf{r})\,\hat{b}_{e\,\mathbf{p}}, \qquad (3)$$

where N is the number of atoms; $\phi_{\text{BEC}}(\mathbf{r})$ is the macroscopically populated BEC wave function normalized as $\int dV |\phi_{\text{BEC}}(\mathbf{r})|^2 = 1$; $\hat{b}_{g\mathbf{p}}$, $\hat{b}_{s\mathbf{p}}$, and $\hat{b}_{e\mathbf{p}}$ are the annihilation operators corresponding to states with atoms in the internal states $|g\rangle$, $|s\rangle$, and $|e\rangle$ and with the external degrees of freedom $\mathbf{p}$; and $\phi_{\mathbf{p}}(\mathbf{r}) \propto e^{i\mathbf{p}\cdot\mathbf{r}}$ are the corresponding motional wave functions which are the momentum eigenfunctions. The

condensate wave function $\phi_{\text{BEC}}(\mathbf{r})$ includes the atom-atom interaction, and it is a broad function filling the trap and having large overlap with the single-particle ground state of the trap and with the zero-momentum eigenfunction $\phi_0(\mathbf{r})$. We can therefore take $\mathbf{p} = 0$ out of the summation over the free motional states for the ground state $|g\rangle$. The tiny overlap with other free motional states with low momentum $\mathbf{p} \approx 0$ can be safely neglected as it has no effect on the forward-photon-scattering amplitude. We can also neglect the influence of the s-wave scattering of free atoms off the condensate. In the following, we will use in place of the zero-momentum wave function $\phi_0(\mathbf{r})$ the BEC wave function $\phi_{\text{BEC}}(\mathbf{r})$ for states $|s\rangle$ and $|e\rangle$. We then obtain the second-quantized Hamiltonian

$$\hat{H} = \sum_{\mathbf{p}}\frac{p^2}{2M}(\hat{b}^{\dagger}_{g\,\mathbf{p}}\hat{b}_{g\,\mathbf{p}} + \hat{b}^{\dagger}_{e\,\mathbf{p}}\hat{b}_{e\,\mathbf{p}}) + \left\{\sqrt{N}\,\eta\,\hat{c}\,\hat{b}^{\dagger}_{s} + \Omega_{\text{d}}\sum_{\mathbf{p}}\hat{b}^{\dagger}_{e\,\mathbf{p}}\hat{b}_{s}\int dV e^{i\mathbf{k}_{\text{d}}\mathbf{r}}\phi^{*}_{\mathbf{p}}(\mathbf{r})\phi_{\text{BEC}}(\mathbf{r})\right.$$

$$+ \sqrt{N}\sum_{\mathbf{p}}\sum_{\mathbf{k},\lambda}\hat{a}_{\mathbf{k},\lambda}\,e^{-i(\omega_k-\omega_{ge})t}\hat{b}^{\dagger}_{e\,\mathbf{p}}\int dV g_{k,\lambda}(\mathbf{r})\phi^{*}_{\mathbf{p}}(\mathbf{r})\phi_{\text{BEC}}(\mathbf{r})$$

$$+ \sum_{\substack{\mathbf{p}\\\mathbf{p}'\neq 0}}\sum_{\mathbf{k},\lambda}\hat{a}_{\mathbf{k},\lambda}\,e^{-i(\omega_k-\omega_{ge})t}\hat{b}^{\dagger}_{e\,\mathbf{p}}\hat{b}_{g\,\mathbf{p}'}\int dV g_{k,\lambda}(\mathbf{r})\phi^{*}_{\mathbf{p}}(\mathbf{r})\phi_{\mathbf{p}'}(\mathbf{r}) + \text{H.c.}\left.\right\}, \qquad (4)$$

where we used the fact that the motional wave functions are the orthonormal eigenfunctions of the kinetic energy and neglected the momentum transfer for the microwave transition $|g\rangle \rightarrow |s\rangle$ leading to the atoms in state $|s\rangle$ having a nonvanishing wave function $\phi_0(\mathbf{r}) \approx \phi_{\text{BEC}}(\mathbf{r})$. Let us confine the description to the single-excitation space, where the state vector of the system can be expanded as

$$|\Psi\rangle = \delta_N|0,0,0\rangle|1_{\text{c}}\rangle|0\rangle + \varsigma_N|0,1,0\rangle|0_{\text{c}}\rangle|0\rangle$$

$$+ \sum_{\mathbf{p}}\epsilon_{N;\mathbf{p}}|0,0,1_{\mathbf{p}}\rangle|0_{\text{c}}\rangle|0\rangle$$

$$+ \sum_{\mathbf{p}'\neq 0}\sum_{\mathbf{k},\lambda}\alpha^{\mathbf{p}'}_{N;\mathbf{k},\lambda}|1_{\mathbf{p}'},0,0\rangle|0_{\text{c}}\rangle|1_{\mathbf{k},\lambda}\rangle$$

$$+ \sum_{\mathbf{k},\lambda}\alpha^{0}_{N;\mathbf{k},\lambda}|0,0,0\rangle|0_{\text{c}}\rangle|1_{\mathbf{k},\lambda}\rangle, \qquad (5)$$

where the five terms on the right-hand side have the following physical meanings:

(i) $|0,0,0\rangle|1_{\text{c}}\rangle|0\rangle$ denotes the state of the system of ultracold atoms in the pure BEC state, a single photon in the microwave resonator, and no photons in the free radiation field.

(ii) $|0,1,0\rangle|0_{\text{c}}\rangle|0\rangle$ denotes the state of the ensemble with a single atom in the internal state $|s\rangle$ due to the absorption of the microwave photon.

(iii) $|0,0,1_{\mathbf{p}}\rangle|0_{\text{c}}\rangle|0\rangle$ denotes the state of the ensemble with a single atom in state $|e\rangle$ with momentum $\mathbf{p}$.

(iv) $|1_{\mathbf{p}'},0,0\rangle|0_{\text{c}}\rangle|1_{\mathbf{k},\lambda}\rangle$ denotes the state of the ensemble with an atom in state $|g\rangle$ having momentum $\mathbf{p}'$, plus an optical photon in the mode with wave vector $\mathbf{k}$ and polarization λ.

(v) $|0,0,0\rangle|0_{\text{c}}\rangle|1_{\mathbf{k},\lambda}\rangle$ denotes a state with all the atoms in the pure BEC state with no excitations, plus an optical photon in the mode with wave vector $\mathbf{k}$ and polarization λ.

Note that the last two states account for the two possible photon emission channels corresponding to the system of ultracold atoms returning to the BEC state $\phi_{\text{BEC}}(\mathbf{r})$ with no excitation (forward scattering) or to a single motional excitation state $\phi_{\mathbf{p}'\neq 0}(\mathbf{r})$ (side scattering), which is illustrated in Fig. 1.

Since the kinetic energy $\frac{p^2}{2M}$ associated with the atomic motion is negligible in comparison to the optical radiation frequencies ω_{c} and ω_{d}, the diagonal terms of Eq. (4) can be omitted.[1] Then the time evolution of the amplitudes is obtained from the Schrödinger equation $i\frac{d|\Psi\rangle}{dt} = \hat{H}|\Psi\rangle$, with the initial conditions $\delta_N(t=0) = 1$ and $\varsigma_N(0) = \epsilon_{N;\mathbf{p}}(0) = \alpha^{\mathbf{p}'\neq 0}_{N;\mathbf{k},\lambda}(0) = \alpha^{0}_{N;\mathbf{k},\lambda}(0) = 0$ for all $\mathbf{p}$, $\mathbf{p}'$, $\mathbf{k}$, and λ, as

$$i\partial_t\delta_N = \sqrt{N}\,\eta^{*}\varsigma_N, \qquad (6a)$$

$$i\partial_t\varsigma_N = \sqrt{N}\,\eta\,\delta_N + \sum_{\mathbf{p}}\epsilon_{N;\mathbf{p}}\,\Omega^{*}_{\text{d}}\int dV e^{-i\mathbf{k}_{\text{d}}\mathbf{r}}\phi_{\mathbf{p}}(\mathbf{r})\phi^{*}_{\text{BEC}}(\mathbf{r}), \qquad (6b)$$

$$i\partial_t\epsilon_{N;\mathbf{p}} = \varsigma_N\,\Omega_{\text{d}}\int dV e^{i\mathbf{k}_{\text{d}}\mathbf{r}}\phi^{*}_{\mathbf{p}}(\mathbf{r})\phi_{\text{BEC}}(\mathbf{r}) + \sum_{\mathbf{p}'\neq 0}\sum_{\mathbf{k},\lambda}\alpha^{\mathbf{p}'}_{N;\mathbf{k},\lambda}$$

$$\times e^{-i(\omega_k-\omega_{ge})t}\int dV g_{k,\lambda}(\mathbf{r})\phi^{*}_{\mathbf{p}}(\mathbf{r})\phi_{\mathbf{p}'}(\mathbf{r})$$

---

[1] $\frac{p^2}{2M}$ can be expressed as $\frac{\omega^2_{\text{d}}}{2Mc^2}$, so the ratio $\frac{p^2/2M}{\omega_{\text{d}}}$ is very small because of the large rest mass of the atoms.

$$
+ \sqrt{N} \sum_{\mathbf{k},\lambda} \alpha_{N;\mathbf{k},\lambda}^0 \, e^{-i(\omega_k - \omega_{ge})t}
$$

$$
\times \int dV g_{k,\lambda}(\mathbf{r}) \phi_{\mathbf{p}}^*(\mathbf{r}) \phi_{\mathrm{BEC}}(\mathbf{r}), \tag{6c}
$$

$$
i\alpha_{N;\mathbf{k},\lambda}^{\mathbf{p}' \neq 0} = \sum_{\mathbf{p}} \int_0^t dt' \epsilon_{N;\mathbf{p}}(t') \, e^{i(\omega_k - \omega_{ge})t'}
$$

$$
\times \int dV g_{k,\lambda}^*(\mathbf{r}) \phi_{\mathbf{p}}(\mathbf{r}) \phi_{\mathbf{p}'}^*(\mathbf{r}), \tag{6d}
$$

$$
i\alpha_{N;\mathbf{k},\lambda}^0 = \sqrt{N} \sum_{\mathbf{p}} \int_0^t dt' \epsilon_{N;\mathbf{p}}(t') \, e^{i(\omega_k - \omega_{ge})t'}
$$

$$
\times \int dV g_{k,\lambda}^*(\mathbf{r}) \phi_{\mathbf{p}}(\mathbf{r}) \phi_{\mathrm{BEC}}^*(\mathbf{r}). \tag{6e}
$$

The first three equations account for the atomic dynamics, while the last two equations describe the generation of the optical radiation field from the atomic source and are integrated to obtain directly the field amplitudes. As seen from Eq. (6e), apart from the nontrivial dependence on N through the amplitude $\epsilon_{N;\mathbf{p}}$, there is a multiplicative factor of $\sqrt{N}$ due to the bosonic enhancement of photoemission when the condensate returns to state $\phi_{\mathrm{BEC}}(\mathbf{r})$.

Our main focus is the spatial profile of the emitted radiation that is collected by Gaussian optics. In Eqs. (6d) and (6e) for the field amplitudes, their spatial profiles are encoded in the overlap integrals and in the amplitudes $\epsilon_{N;\mathbf{p}}(t)$, where the latter also depends on time. At this point, concerning Eqs. (6), there are two ways to treat this problem: one which can handle the general case, where the time and spatial dependence of the amplitudes are not necessarily separable, and which is demanding to solve numerically because we have a continuum set of momentum states and one which solves analytically the equations of motion in certain limits in such a way that the amplitudes become separable in their time and spatial variables. In this work we choose the second implementation because we are interested in how the geometrical parameters affect the incoupled photon rate, regardless of the internal dynamics of the system.

To this end, we separate the temporal and spatial dependences in these formulas; we have to separate the temporal and wave-vector dependences of the amplitudes $\epsilon_{N;\mathbf{p}}(t)$. This is a good approximation in the perturbative limit, considering a short time at the beginning of the process, when the time evolution (6a)–(6c) can be approximated by the content of the initially fully occupied amplitude δ_N being transferred into the initially empty amplitudes ς_N and $\epsilon_{N;\mathbf{p}}$:

$$
i\partial_t \varsigma_N \approx \sqrt{N}\eta(t), \tag{7a}
$$

$$
i\partial_t \epsilon_{N;\mathbf{p}} \approx \varsigma_N \, \Omega_{\mathrm{d}}(t) \int dV e^{i\mathbf{k}_{\mathrm{d}}\mathbf{r}} \phi_{\mathbf{p}}^*(\mathbf{r}) \phi_{\mathrm{BEC}}(\mathbf{r}), \tag{7b}
$$

where Eq. (6a) is eliminated, with δ_N being treated simply as a decaying amplitude, and we introduced the time-dependent drive $\eta(t)$ by the product of the microwave coupling strength η and the depleting initial-state amplitude δ_N. We assumed that during this short period, in the time evolution of ς_N and $\epsilon_{N;\mathbf{p}}$ only the first, leading-order terms will contribute. Performing the time integration, the amplitude corresponding
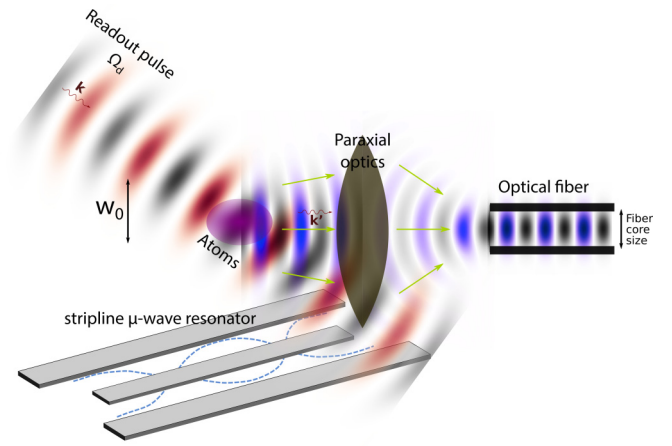

FIG. 2. The geometry of the system of atoms, paraxial optics, and the fiber.

to the intermediate state $\{|e\rangle; \mathbf{p}\}$ reads

$$
\epsilon_{N;\mathbf{p}}(t) \approx -\sqrt{N} \int_0^t \int_0^{t'} dt' dt'' \Omega_{\mathrm{d}}(t')\eta(t'')
$$

$$
\times \int dV e^{i\mathbf{k}_{\mathrm{d}}\mathbf{r}} \phi_{\mathbf{p}}^*(\mathbf{r}) \phi_{\mathrm{BEC}}(\mathbf{r})
$$

$$
\equiv \sqrt{N} \, \epsilon(t) \int dV e^{i\mathbf{k}_{\mathrm{d}}\mathbf{r}} \phi_{\mathbf{p}}^*(\mathbf{r}) \phi_{\mathrm{BEC}}(\mathbf{r})
$$

$$
= \sqrt{N} \frac{\epsilon(t)}{\sqrt{V}} \int dV e^{i\mathbf{k}_{\mathrm{d}}\mathbf{r}} e^{-i\mathbf{p}\mathbf{r}} \phi_{\mathrm{BEC}}(\mathbf{r})
$$

$$
= \sqrt{N} \frac{\epsilon(t)}{\sqrt{V}} \tilde{\phi}_{\mathrm{BEC}}(\mathbf{p} - \mathbf{k}_{\mathrm{d}}), \tag{8}
$$

where we used the momentum eigenstates $1/\sqrt{V} \, e^{i\mathbf{p}\mathbf{r}}$ for the wave function of the intermediate states, we denoted the Fourier transform of ϕ_{BEC} by $\tilde{\phi}_{\mathrm{BEC}}$, and we have factorized the N and wave-number $\mathbf{p}$ dependence out of the amplitude $\epsilon_{N;\mathbf{p}}(t)$ by introducing $\epsilon(t)$, depending only on time.

Hereafter, we focus on the spatial profile of the generated radiation and on the atom-number dependence of the process: calculating the photon rate of the two channels defined in Eqs. (6d) and (6e) and coupled into an optical fiber, using the amplitude $\epsilon_{N;\mathbf{p}}$ from Eq. (8) for the $|g\rangle \rightarrow \{|e\rangle; \mathbf{p}\}$ part of the photon conversion.

III. RADIATION INTO GAUSSIAN MODES

The aim is to collect the emitted radiation into an optical fiber. The modes of a single-mode fiber form a one-dimensional manifold which can be parametrized by a scalar wave number k. The important parameters are the size of the fiber core and the orientation of the fiber with respect to the axis of the driving field that determines the phase-matched emission direction. To model the incoupling process, we assume a generic paraxial optical array, which transforms a set of free, nearly paraxial beams to the strongly confined guided mode (see Fig. 2). The fiber modes confined in the core of size d_{core} are transformed in free space to Gaussian modes with waist w_0 determined by the parameters of the optical array at

the position of the ensemble:[2]

$$d_{\text{core}}, k \quad @ \text{ fiber entrance}$$
$$\Longleftrightarrow w_0, k \quad @ \text{ position of the BEC.}$$

On the basis of the foregoing considerations, from the full set of free-space modes we can separate a set of guided modes with wave vectors aligned with the axis of the fiber that are coupled by the optical array into the fiber. These modes can be well approximated by Gaussian modes with wave number k and waist w_0, with mode function

$$
\begin{aligned}
f_k(\mathbf{r}) &= \frac{z_{\text{R}}}{q^*(z)} \exp\left(ik\left[z + \frac{\rho^2}{2\, q^*(z)} \right] \right) \\
&= i \frac{w_0}{w(z)} \exp\left[ikz - \frac{\rho^2}{w(z)^2} \right. \\
&\quad \left. + i\frac{k\rho^2}{2R(z)} - i\phi_{\text{Gouy}} \right] \equiv \varphi_{\text{G}}(\mathbf{r})\, e^{ikz},
\end{aligned}
\tag{9}
$$

where z is the position along the direction of the fiber axis, $\rho = \sqrt{x^2 + y^2}$ is the radial coordinate, $q(z) = z + iz_{\text{R}}$ is the complex beam parameter with the Rayleigh range $z_{\text{R}} = kw_0^2/2$, $w(z) = w_0\sqrt{1 + z^2/z_{\text{R}}^2}$ is the transverse beam size, $R(z) = z + z_{\text{R}}^2/z$ is the radius of curvature of the wave front, and $\phi_{\text{Gouy}} = \arctan(z/z_{\text{R}})$ is the Gouy phase. For a given optical array, with a well-defined beam waist w_0 and axis, we can claim that the set of Gaussian modes parametrized by k forms an orthonormal set, which is important to ensure the correct commutation relation for the electric field. The amplitudes of the guided modes corresponding to the N- and $\mathbf{p}'$-dependent free-space amplitudes $\alpha_{N;\mathbf{k},\lambda}^{\mathbf{p}'\neq0}$ and $\alpha_{N;\mathbf{k},\lambda}^0$ are denoted by $\beta_{N;\mathbf{k},\lambda}^{\mathbf{p}'\neq0}$ and $\beta_{N;\mathbf{k},\lambda}^0$. The β amplitudes simply replace the α's in Eqs. (6) in the case when all electromagnetic processes are confined to the guided modes.

The expectation value of the positive-frequency part of the electric field that is coupled into the fiber reads

$$
\mathbf{E}_{\text{G}}^+(\mathbf{r}) = i \sum_{\mathbf{p}'} \sum_{k,\lambda} \sqrt{\frac{\omega}{2\varepsilon_0 V}}\, \beta_{N;k,\lambda}^{\mathbf{p}'}(t)\, \mathbf{e}_\lambda\, f_k(\mathbf{r}),
\tag{10}
$$

where $V = \mathcal{A}L$ is the mode volume, with $\mathcal{A} = \pi w_0^2/4$ being its cross-sectional area and L being the fictitious quantization length along the propagation axis, and there is a sum for all subchannels labeled by all the possible momenta $\mathbf{p}'$; with the BEC acting as a momentum reservoir, there is no constraint for the absorbable momentum $\mathbf{p}'$. The fiber-coupled modes form a broadband continuum, and the field $\mathbf{E}_{\text{G}}$ can be treated similarly to that of the three-dimensional electromagnetic vacuum surrounding the atom [47]. Irreversible photon emission from an excited-state atom into the fiber takes place, and the photon emission rate is determined by the local coupling

___

between the atom and the modes,

$$
g_{k,\lambda}(\mathbf{r}_{\text{A}}) = \sqrt{\frac{\omega}{2\varepsilon_0 V}}\, \mathbf{d}_{ge}\mathbf{e}_\lambda\, f_k(\mathbf{r}_{\text{A}}) = g_{k,\lambda}\, f_k(\mathbf{r}_{\text{A}}).
\tag{11}
$$

When the newly introduced amplitudes $\beta_{N;k,\lambda}^{\mathbf{p}'\neq0}$ and $\beta_{N;k,\lambda}^0$ replace the corresponding α's in Eqs. (6d) and (6e), the coupling constants have to be written as Eq. (11).

The total photon numbers generated during a small time interval Δt, denoted $\Delta n(t)$ and $\Delta n^0(t)$ in the side- and forward-scattering channels, respectively, read

$$
\begin{aligned}
\Delta n(t) &= \sum_{\mathbf{p}'\neq0} \sum_{k,\lambda} \left| \Delta \beta_{N;k,\lambda}^{\mathbf{p}'}(t) \right|^2 \\
&= \sum_{\mathbf{p}'\neq0} \sum_{k,\lambda} \left| \int_{t-\Delta t}^{t} dt'\, \beta_{N;k,\lambda}^{\mathbf{p}'}(t') \right|^2,
\end{aligned}
\tag{12a}
$$

$$
\begin{aligned}
\Delta n^0(t) &= \sum_{k,\lambda} \left| \Delta \beta_{N;k,\lambda}^0(t) \right|^2 \\
&= \sum_{k,\lambda} \left| \int_{t-\Delta t}^{t} dt'\, \beta_{N;k,\lambda}^0(t') \right|^2.
\end{aligned}
\tag{12b}
$$

A. Free final state of the atom

Let us first consider the case when the ensemble of ultracold atoms excited into state $|e\rangle$, on emitting a photon, does not return to the BEC state $\phi_{\text{BEC}}(\mathbf{r})$ but ends up in an arbitrary free state with momentum $\mathbf{p}'$ (side scattering). The total photon number $\Delta n(t)$ according to Eq. (12a) reads

$$
\begin{aligned}
\Delta n(t) &= \sum_{\mathbf{p}'} \sum_{k,\lambda} \left| \Delta \beta_{N;k,\lambda}^{\mathbf{p}'}(t) \right|^2 \\
&= \sum_{\mathbf{p}'} \sum_{\mathbf{p}_1,\mathbf{p}_2} \sum_{k,\lambda} |g_{k,\lambda}|^2 \int_{t-\Delta t}^{t} dt_1 \epsilon_{N;\mathbf{p}_1}^*(t_1)\, e^{i(\omega_k - \omega_{ge})(t-t_1)} \\
&\quad \times \int_{t-\Delta t}^{t} dt_2\, \epsilon_{N;\mathbf{p}_2}(t_2)\, e^{i(\omega_k - \omega_{ge})(t_2-t)} \int dV f_k(\mathbf{r})\phi_{\mathbf{p}_1}^*(\mathbf{r}) \\
&\quad \times \phi_{\mathbf{p}'}(\mathbf{r}) \int dV' f_k^*(\mathbf{r}')\phi_{\mathbf{p}_2}(\mathbf{r}')\phi_{\mathbf{p}'}^*(\mathbf{r}'),
\end{aligned}
\tag{13}
$$

where for the amplitudes $\beta_{N;k,\lambda}^{\mathbf{p}'}(t)$ we used Eq. (6d) with the coupling constants $g_{k,\lambda}(\mathbf{r})$ defined in Eq. (11). The coupling constant $g_{k,\lambda}$ is a flat function of the wave number k, whereas the overlap integrals [the last two terms of Eq. (13)] result in a function which has a bandwidth $1/\Lambda$, where Λ is the characteristic length corresponding to the BEC. However, the summation over all possible final momenta $\mathbf{p}'$ ensures that the fiber-coupled modes form a broadband continuum around the transition frequency ω_{ge} with a bandwidth much larger than the inverse of the short time interval Δt. We also assume weak coupling and neglect the reabsorption of photons within the cloud. The summation over the wave number k together with the time integrals thus creates a situation analogous to the calculation of spontaneous emission in the three-dimensional free-space modes. Hence, we can adopt the Born-Markov approximation to evaluate the sum in Eq. (13). Because of the broadband summation over k of the exponential terms $e^{i(\omega_k - \omega_{ge})(t_2-t_1)}$, only the time instant $t_1 \approx t_2$ contributes to the

combined summation over k and the time integrals over $t_{1,2}$. The atomic amplitudes $\epsilon(t_{1,2})$ are thus taken at the same time, and furthermore, because the variation in the period Δt is infinitesimal, both amplitudes can be replaced by $\epsilon(t)$

and taken out of the time integrals. The remaining time integrals can be carried out, one of them giving a Dirac δ in frequency space and the other one being simply Δt, as follows:

$$
\begin{aligned}
\Delta n(t) &\approx N \sum_{\mathbf{p}'} \sum_{\mathbf{p}_1,\mathbf{p}_2} \epsilon_{N;\mathbf{p}_1}^*(t)\epsilon_{N;\mathbf{p}_2}(t) \sum_{k,\lambda} |g_{k,\lambda}|^2 \int_{t-\Delta t}^{t} dt_1 \int_{t-\Delta t}^{t} dt_2 e^{i(\omega_k-\omega_{ge})(t_2-t_1)} \\
&\quad \times \int dV f_k(\mathbf{r})\phi_{\mathbf{p}_1}^*(\mathbf{r})\phi_{\mathbf{p}'}(\mathbf{r}) \int dV' f_k^*(\mathbf{r}')\phi_{\mathbf{p}_2}(\mathbf{r}')\phi_{\mathbf{p}'}^*(\mathbf{r}') \\
&= N \sum_{\mathbf{p}'} \sum_{\mathbf{p}_1,\mathbf{p}_2} \epsilon_{N;\mathbf{p}_1}^*(t)\epsilon_{N;\mathbf{p}_2}(t) \sum_{\lambda} \frac{L}{2\pi} \int dk \frac{\omega_k}{2\varepsilon_0 V}(\mathbf{d}_{ge}\mathbf{e}_\lambda)^2 \Delta t\, 2\pi \delta(\omega_k-\omega_{ge}) \\
&\quad \times \int dV f_k(\mathbf{r})\phi_{\mathbf{p}_1}^*(\mathbf{r})\phi_{\mathbf{p}'}(\mathbf{r}) \int dV' f_k^*(\mathbf{r}')\phi_{\mathbf{p}_2}(\mathbf{r}')\phi_{\mathbf{p}'}^*(\mathbf{r}') \\
&= N \Gamma \frac{\sigma_{\mathrm{A}}}{\mathcal{A}} \Delta t \sum_{\mathbf{p}'} \left| \sum_{\mathbf{p}} \epsilon_{N;\mathbf{p}}(t) \int dV f_{k_{ge}}^*(\mathbf{r})\phi_{\mathbf{p}}(\mathbf{r})\phi_{\mathbf{p}'}^*(\mathbf{r}) \right|^2 .
\end{aligned}
\tag{14}
$$

Here the sum over the polarization λ was simplified by assuming the optimum configuration: the driving laser is linearly polarized perpendicular to the plane of Fig. 2, i.e., the plane spanned by the propagation of the driving laser beam $\mathbf{k}_d$ and the fiber-coupled modes. The induced atomic dipole moment $\mathbf{d}_{ge}$ then has the same out-of-plane direction. One of the two possible polarizations of the fiber-coupled modes is also perpendicular to this plane and hence is parallel to the dipole moment $\mathbf{d}_{ge}$. The other one is in plane, being orthogonal and thus decoupled from the atomic dipole. The remaining deriva-

tion follows the standard Born-Markov (Wigner-Weisskopf) procedure. We identify the free-space atomic spontaneous emission rate $\Gamma = \omega_{ge}^3 d_{ge}^2/(6\pi\varepsilon_0 c^3)$ and the radiative cross section of the atomic dipole $\sigma_{\mathrm{A}} = 3\lambda^2/(2\pi)$ in order to put the final result in a compact form.

Using the approximation (8) for the amplitudes $\epsilon_{N;\mathbf{p}}(t)$, the rate of photons $I = \Delta n/\Delta t$ coupled into the fiber is

$$
\begin{aligned}
I(t) &= N \Gamma |\epsilon(t)|^2 \frac{\sigma_{\mathrm{A}}}{\mathcal{A}} \sum_{\mathbf{p}'} \left| \frac{1}{V\sqrt{V}} \sum_{\mathbf{p}} \tilde{\phi}_{\mathrm{BEC}}(\mathbf{p}-\mathbf{k}_d) \int dV \varphi_{\mathrm{G}}^*(\mathbf{r}) e^{i(\mathbf{p}-\mathbf{k}_{ge}-\mathbf{p}')\mathbf{r}} \right|^2 \\
&= N \Gamma |\epsilon(t)|^2 \frac{\sigma_{\mathrm{A}}}{\mathcal{A}} \sum_{\mathbf{p}'} \left| \int dV \frac{1}{\sqrt{V}} \phi_{\mathrm{BEC}}(\mathbf{r})\varphi_{\mathrm{G}}^*(\mathbf{r}) e^{i(\mathbf{k}_d-\mathbf{k}_{ge}-\mathbf{p}')\mathbf{r}} \right|^2 \\
&= N \Gamma |\epsilon(t)|^2 \frac{\sigma_{\mathrm{A}}}{\mathcal{A}} \int dV |\phi_{\mathrm{BEC}}(\mathbf{r})\varphi_{\mathrm{G}}(\mathbf{r})|^2 \equiv N \Gamma |\epsilon(t)|^2 \frac{\sigma_{\mathrm{A}}}{\mathcal{A}} \xi .
\end{aligned}
\tag{15}
$$

We thus find that the photon-scattering rate into the fiber is proportional to (i) the number of atoms N, (ii) the single-atom photon-scattering rate $\Gamma |\epsilon(t)|^2$ in the full solid angle, (iii) the ratio of the atomic radiative cross section and the cross section of the fiber-coupled beam, and (iv) a geometrical factor ξ which includes the nontrivial condition on the spatial matching of light beams and the atom cloud.

It is remarkable that, in the plane of the driving laser and the fiber-coupled mode, the intensity $I(t)$ is independent of the angle between the wave vector $\mathbf{k}_d$ and the fiber axis. The reason is that momentum conservation in the photon-scattering process is not restrictive in the case of a BEC initial state of the atomic ensemble. Due to its extremely flat dispersion

relation compared to that of the photons, the BEC acts as a momentum reservoir that can absorb away any momentum mismatch without significantly altering the energetics of the photon-scattering process. A broad angular distribution has a significant consequence in practical applications: the generated photon can be easily separated from the driving laser beam, without the need for narrowband spectral filters, which necessarily degrade the coupling efficiency into the fiber. We note that this isotropic distribution (or dipole pattern in the case of a fixed direction of the atomic dipole moments) holds only for the first photon; already, the second photon, encountering the Bragg grating created by the excitation left by the first photon, will preferentially scatter in the same direction [48].

B. BEC final state of the atom

A case of special interest is when the final state of the atoms after the photon emission coincides with the BEC state as in the beginning. Although the final state is now a single motional state $\phi_{\rm BEC}$ and not a broad continuum, the scattered intensity is sizable because of the bosonic enhancement. The probability of this transition is strongly enhanced by the macroscopic part of the atomic population in the BEC state. The generated field amplitude in the fiber is given by Eq. (6e). When going through the same steps as in Eqs. (14) and (15) to get $\Delta n^0(t)$, extra care must be taken in applying the Born-Markov approximation. Unlike the previous case of a free final state, now there is no summation over the broadband continuum of momentum states p', i.e.,

$$
\begin{aligned}
\Delta n^0(t) &= \sum_{k,\lambda} \left| \Delta \beta^0_{N;k,\lambda}(t) \right|^2 \\
&= \sum_{\mathbf{p}_1,\mathbf{p}_2} \sum_{k,\lambda} |g_{k,\lambda}|^2 \int_{t-\Delta t}^{t} dt_1 \epsilon^*_{N;\mathbf{p}_1}(t_1) \, e^{i(\omega_k - \omega_{ge})(t-t_1)} \\
&\quad \times \int_{t-\Delta t}^{t} dt_2 \epsilon_{N;\mathbf{p}_2}(t_2) \, e^{i(\omega_k - \omega_{ge})(t_2-t)} \int dV f_k(\mathbf{r}) \\
&\quad \times \phi^*_{\mathbf{p}_1}(\mathbf{r}) \phi_{\rm BEC}(\mathbf{r}) \int dV' f^*_k(\mathbf{r}') \phi_{\mathbf{p}_2}(\mathbf{r}') \phi^*_{\rm BEC}(\mathbf{r}').
\end{aligned}
\tag{16}
$$

The wave-number summation has a finite support which originates from the overlap integrals. Physically, this bandwidth is determined by (i) the width $1/\Lambda$ of the BEC wave function in momentum space and (ii) the width of the intermediate states $p_{1,2}$. The latter incorporates the drive-laser pulse width and the BEC bandwidth. The Born-Markov approximation can be adopted to simplify the above equation if the characteristic timescale to generate a photon in this four-wave mixing process is much longer than the correlation time τ_c where $(c\tau_c)^{-1}$ is the effective bandwidth of the fiber mode continuum just discussed. Under this condition, the intensity in this photon-scattering channel reads

$$
\begin{aligned}
I_0(t) &= \sum_{k,\lambda} \left| \Delta \beta^0_{N;k,\lambda}(t) \right|^2 / \Delta t \\
&= N^2 \, \Gamma \, |\epsilon(t)|^2 \, \frac{\sigma_{\rm A}}{\mathcal{A}} \left| \int dV |\phi_{\rm BEC}(\mathbf{r})|^2 \varphi^*_{\rm G}(\mathbf{r}) e^{i(\mathbf{k}_{\rm d} - \mathbf{k}_{ge})\mathbf{r}} \right|^2 \\
&\equiv N^2 \, \Gamma \, |\epsilon(t)|^2 \, \frac{\sigma_{\rm A}}{\mathcal{A}} \, |\xi_0|^2.
\end{aligned}
\tag{17}
$$

Note that the intensity scales now quadratically with the number of atoms, while the geometric factor ξ_0 involves the BEC wave function in a different power compared to Eq. (15). Moreover, the geometric factor is no longer isotropic: there is no momentum transfer to the final BEC state that would compensate the momentum mismatch of the readout and emitted photon, so the outgoing photon has to take the momentum of the absorbed photon from the driving laser, resulting in predominantly forward scattering. This result for the photon-scattering rate allows for justifying the validity of the Born-Markov approximation *a posteriori*. If the photon generation process in the forward direction becomes very efficient, i.e., $I_0 \tau_c \sim 1$, the Born-Markov approximation breaks down. This can happen, for example, for a large number of atoms. The underlying physical picture is that the photon reabsorption cannot be neglected for the case of strong coupling between the BEC and the optical modes. However, this is a favorable case in which the optical photon can be generated on a short timescale by means of an appropriate laser pulse.

C. Analytical approximations for the scattered intensity

In order to proceed with analytic expressions, we approximate the BEC wave function by a Gaussian corresponding to the ground state of a noninteracting gas in a harmonic trap with cylindrical symmetry,

$$
\phi_{\rm BEC}(\mathbf{r}) = \frac{1}{(2\pi)^{3/4} \, \sigma \sigma_z^{1/2}} \exp\left(-\frac{x^2+y^2}{4\sigma^2} - \frac{z^2}{4\sigma_z^2} \right), \tag{18}
$$

where $\sigma_x = \sigma_y = \sigma$ and σ_z are the oscillator lengths of the trap. We consider the configuration in which the axis of the optical fiber coincides with the long axis of the condensate (see Fig. 2), characterized by the oscillator length σ_z. In the case of a free-atom final state, the geometric factor ξ reads

$$
\begin{aligned}
\xi &= \int dV |\phi_{\rm BEC}(\mathbf{r}) \varphi_{\rm G}(\mathbf{r})|^2 \\
&= \frac{w_0^2}{(2\pi)^{3/2} \sigma^2 \sigma_z} \int dV \frac{1}{w(z)^2} \\
&\quad \times \exp\left[-\frac{x^2+y^2}{2}\left(\frac{1}{\sigma^2} + \frac{1}{w(z)^2} \right) - \frac{z^2}{2\sigma_z^2} \right] \\
&= \frac{w_0^2}{\sqrt{2\pi}\sigma_z} \int dz \frac{\exp\left(-\frac{z^2}{2\sigma_z^2}\right)}{\sigma^2 + w(z)^2} \approx \frac{w_0^2}{\sigma^2 + w_0^2},
\end{aligned}
\tag{19}
$$

where the last approximation is valid in the typical case when the longitudinal length σ_z of the condensate is much smaller than the Rayleigh range, so that the transverse beam size $w(z)$ can be approximated by the beam waist w_0. The result shows that the geometrical factor $\xi \lesssim 1$. The larger the beam waist is, the better the geometrical coupling factor is. This is reasonable as the optics that couples into the fiber collects light from a larger solid angle.

If the ensemble of ultracold atoms returns to the BEC state, the geometric factor, within the same approximations, is

$$
\begin{aligned}
\xi_0(\theta) &= \int dV |\phi_{\rm BEC}(\mathbf{r})|^2 \varphi^*_{\rm G}(\mathbf{r}) e^{i(\mathbf{k}_{\rm d} - \mathbf{k}_{ge})\mathbf{r}} \\
&= \frac{z_{\rm R}}{(2\pi)^{3/2}\sigma^2 \sigma_z} \int dV \frac{1}{q(z)} \\
&\quad \times \exp\left[-\frac{x^2+y^2}{2}\left(\frac{1}{\sigma^2} + i\frac{k_{\rm d}}{q(z)} \right) \right. \\
&\quad \left. -\frac{z^2}{2\sigma_z^2} + ik_{\rm d}(\cos\theta - 1)z + ik_{\rm d}\sin\theta \, x \right] \\
&= \frac{z_{\rm R}}{\sqrt{2\pi}\sigma_z} \int dz \frac{1}{q(z) + ik_{\rm d}\sigma^2} \exp\left[-\frac{ik_{\rm d}^2 \sigma^2 q(z)}{2(q(z) + ik_{\rm d}\sigma^2)} \right. \\
&\quad \left. \times \sin^2\theta + ik_{\rm d}(\cos\theta-1)z - \frac{z^2}{2\sigma_z^2} \right],
\end{aligned}
\tag{20}
$$

where θ is the angle between the direction of the incoming driving field $\mathbf{k}_d$ and the direction of the optical fiber $\mathbf{k}$. For the forward-scattering direction, $\theta = 0$, which was already calculated in [22], we have

$$
\begin{aligned}
\xi_0 &= \frac{z_R}{(2\pi)^{3/2}\sigma^2\sigma_z} \int dV \frac{1}{q(z)} \\
&\quad \times \exp\left[-\frac{x^2+y^2}{2}\left(\frac{1}{\sigma^2} + i\frac{k_d}{q(z)}\right) - \frac{z^2}{2\sigma_z^2} \right] \\
&= -i\sqrt{\frac{\pi}{2}}\frac{z_R}{\sigma_z} e^{\frac{(z_R+k_d\sigma^2)^2}{2\sigma_z^2}} \operatorname{erfc}\left(\frac{z_R + k_d\sigma^2}{\sqrt{2}\sigma_z}\right) \\
&\approx \frac{w_0^2}{2\sigma^2 + w_0^2},
\end{aligned}
\tag{21}
$$

where in last line we again used the approximation that the longitudinal length σ_z of the condensate is much smaller than the Rayleigh range z_R.

So far we have seen that for every $(\mathbf{k}_d, \mathbf{k}_{ge})$ the radiation collected by the Gaussian optics has two components: one which is independent of the angle θ and is proportional to N and one which is confined to a small solid angle around $\theta = 0$ and is proportional to N^2. Certainly, the latter dominates the photon emission in the forward direction for a sufficiently large atom number.

IV. NUMERICAL RESULTS AND DISCUSSION

We consider a cylindrically symmetric harmonic trap and an optical fiber oriented in the z direction and address the question of which part of the incoupled intensity, Eq. (15) or Eq. (17), gives the larger contribution to the collected radiation for a given trap geometry σ, σ_z and beam waist w_0 at different angles θ. It was already shown in [22] that the intensity of the forward scattering is optimized if the beam waist equals $\sqrt{2}\sigma$. So in the following we are going to fix $w_0 = \sqrt{2}\sigma$. In the limit of small longitudinal size relative to the Rayleigh range, the geometrical factors (19) and (21) become $\xi = 2/3$ and $|\xi_0|^2 = 1/4$, respectively. To compare the two radiation channels, we study the distinct parts of the intensities (15) and (17), namely, the geometrical factors $|\xi_0(\theta)|^2$ and ξ/N (see Fig. 3), with dimensionless quantities defined as $\overline{\sigma} = k_d\sigma$, $\overline{\sigma}_z = k_d\sigma_z$, and $\overline{w}_0 = k_d w_0$.

If the BEC has an oblate or a nearly spherical shape, the superradiant part of the geometrical factor takes a maximum value of $1/4$ in the forward direction $\theta = 0$, while the isotropic channel results in $\xi = 2/3$. In this case $\overline{\sigma}^2 > \overline{\sigma}_z$, which is equivalent to the setup in which the Rayleigh range is much larger than the longitudinal size σ_z. As the spheroid becomes prolate and σ_z becomes comparable to z_R, the geometrical factors of both channels decrease. At a certain point where the shape of the BEC becomes very elongated, the maximum of the anisotropic radiation is displaced to a nontrivial angle. The reason for this is that the curvature and the Gouy phase term of the Gaussian beam become significant, which can be compensated for in Eq. (20) only by a nonzero θ.

Around $\theta = 0$ the dominant contribution comes from superradiant emission from the BEC, but above a particular angle θ^*, which depends on the trap geometry, the isotropic
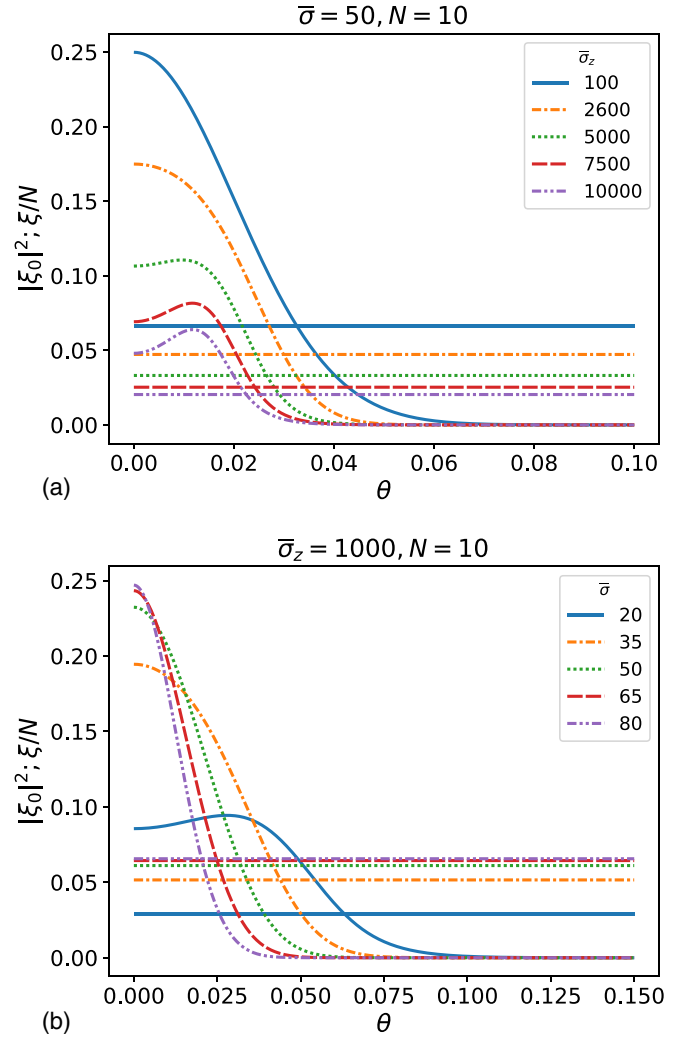

FIG. 3. Angular dependence of the geometrical factor $|\xi_0(\theta)|^2$ (curves) corresponding to the superradiance and the value of the geometrical factor ξ/N (horizontal lines) for the isotropic radiation for a fixed number of atoms $N = 10$ for various values of (a) the transverse size $\overline{\sigma}_z$ and (b) the longitudinal size $\overline{\sigma}$. θ is measured in radians.

radiation exceeds the superradiant one. This critical angle increases if the geometrical parameters σ and σ_z decrease.

For a small number of atoms, only the isotropic part is significant for nearly all angles θ (see Fig. 4). But as the number of atoms increases, the superradiance becomes important in an ever-widening range around the forward direction, as it is amplified by a factor of N compared to the isotropic radiation.

Finally, we make some remarks about the possibility of converting microwave photons to optical ones with the present scheme. The efficiency of such a process is ultimately determined by how valid the simplifying assumptions made in our modeling are in an experiment and at what rate technical imperfections enter. Indeed, if we assume that a single excitation in the microwave mode $\hat{c}$ has an infinite lifetime and the whole scheme can be maintained indefinitely, then, however slowly, the microwave photon will always be transformed into an emitted optical photon by the system leaking through states
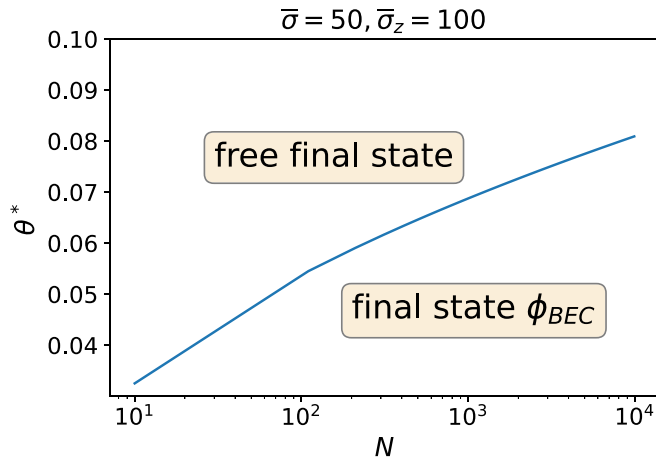
FIG. 4. The dependence of the critical angle θ^* (the two channels have the same contribution) on the atom number N for fixed geometry $\overline{\sigma} = 50$, $\overline{\sigma}_z = 100$. θ^* is measured in radians.

$|s\rangle$ and $|e\rangle$ and ending up back in $|g\rangle$ after what is essentially a two-photon optical pumping process. The real question is therefore not the efficiency but the rate of the conversion, which needs to be higher than the rate at which the conditions degrade in an experiment or factors excluded from our model come into play. According to Eqs. (15) and (17), the photon-creation rate is proportional to the rate of populating state $|e\rangle$. Optimizing this is analogous to population transfer: one has to optimize the shape of the pulse $\Omega_d(t)$ with respect to the pulse $\eta(t)$, that is, the temporal envelope of the microwave photon interacting with the atom. Compared to conventional EIT and STIRAP schemes, here the optimization problem is complicated by the presence of a continuum of momentum states of the BEC.

V. CONCLUSIONS

To summarize, we have considered the photon emission by a Raman process with Λ atoms in a BEC. In addition to the internal atomic state, we have taken into account the atomic external, motional degree of freedom in order to describe the momentum transfer in the photon recoil. We performed the analysis in the perturbative, weak-excitation limit, in which we were able to separate the spatial dependence of the emitted radiation from its temporal dynamics. Under these approximations, we have shown that there are two channels for the converted radiation: the superradiant one, which corresponds to the phase-matched photon scattering in the forward direction, and the isotropic one, in which the Bose-Einstein condensate takes away an arbitrary momentum mismatch between the incoming and emitted radiation. The contribution of the latter is more significant in the side-scattering directions, while the width of this region varies with the number of atoms in the condensate and with the dimensions of the harmonic trap.

[1] H. J. Kimble, Nature (London) **453**, 1023 (2008).

[2] R. van Meter, *Quantum Networking* (Wiley, Hoboken, NJ, 2014).

[3] D. Awschalom *et al.*, PRX Quantum **2**, 017002 (2021).

[4] L. M. K. Vandersypen and I. L. Chuang, Rev. Mod. Phys. **76**, 1037 (2005).

[5] J. Schupp, V. Krcmarsky, V. Krutyanskiy, M. Meraner, T. E. Northup, and B. Lanyon, PRX Quantum **2**, 020331 (2021).

[6] A. Heinz, A. J. Park, N. Šantić, J. Trautmann, S. G. Porsev, M. S. Safronova, I. Bloch, and S. Blatt, Phys. Rev. Lett. **124**, 203201 (2020).

[7] A. Reiserer and G. Rempe, Rev. Mod. Phys. **87**, 1379 (2015).

[8] P. Lodahl, S. Mahmoodian, and S. Stobbe, Rev. Mod. Phys. **87**, 347 (2015).

[9] P. Senellart, G. Solomon, and A. White, Nat. Nanotechnol. **12**, 1026 (2017).

[10] N. Kalb, A. A. Reiserer, P. C. Humphreys, J. J. W. Bakermans, S. J. Kamerling, N. H. Nickerson, S. C. Benjamin, D. J. Twitchen, M. Markham, and R. Hanson, Science **356**, 928 (2017).

[11] F. Arute *et al.*, Nature (London) **574**, 505 (2019).

[12] A. Blais, A. L. Grimsmo, S. M. Girvin, and A. Wallraff, Rev. Mod. Phys. **93**, 025005 (2021).

[13] N. Lauk, N. Sinclair, S. Barzanjeh, J. P. Covey, M. Saffman, M. Spiropulu, and C. Simon, Quantum Sci. Technol. **5**, 020501 (2020).

[14] M. Forsch, R. Stockill, A. Wallucks, I. Marinković, C. Gärtner, R. A. Norte, F. van Otten, A. Fiore, K. Srinivasan, and S. Gröblacher, Nat. Phys. **16**, 69 (2020).

[15] A. Vainsencher, K. Satzinger, G. Peairs, and A. Cleland, Appl. Phys. Lett. **109**, 033107 (2016).

[16] K. C. Balram, M. I. Davanço, J. D. Song, and K. Srinivasan, Nat. Photonics **10**, 346 (2016).

[17] N. J. Lambert, A. Rueda, F. Sedlmeir, and H. G. L. Schwefel, Adv. Quantum Technol. **3**, 1900077 (2020).

[18] A. P. Higginbotham, P. Burns, M. Urmey, R. Peterson, N. Kampel, B. Brubaker, G. Smith, K. Lehnert, and C. Regal, Nat. Phys. **14**, 1038 (2018).

[19] W. Jiang, C. J. Sarabalis, Y. D. Dahmani, R. N. Patel, F. M. Mayor, T. P. McKenna, R. Van Laer, and A. H. Safavi-Naeini, Nat. Commun. **11**, 1166 (2020).

[20] M. Mirhosseini, A. Sipahigil, M. Kalaee, and O. Painter, Nature (London) **588**, 599 (2020).

[21] G. Arnold, M. Wulf, S. Barzanjeh, E. Redchenko, A. Rueda, W. J. Hease, F. Hassani, and J. M. Fink, Nat. Commun. **11**, 4460 (2020).

[22] Á. Kurkó, P. Domokos, A. Vukics, T. Bækkegaard, N. T. Zinner, J. Fortágh, and D. Petrosyan, EPJ Quantum Technol. **8**, 11 (2021).

[23] Z. Peng, S. De Graaf, J. Tsai, and O. Astafiev, Nat. Commun. **7**, 12588 (2016).

[24] Y. Zhou, Z. Peng, Y. Horiuchi, O. V. Astafiev, and J. S. Tsai, Phys. Rev. Applied **13**, 034007 (2020).

[25] M. Fleischhauer, A. Imamoglu, and J. P. Marangos, Rev. Mod. Phys. **77**, 633 (2005).

[26] K. Hammerer, A. S. Sørensen, and E. S. Polzik, Rev. Mod. Phys. **82**, 1041 (2010).

[27] J. P. Covey, A. Sipahigil, and M. Saffman, Phys. Rev. A **100**, 012307 (2019).

[28] D. Petrosyan, K. Mølmer, J. Fortágh, and M. Saffman, New J. Phys. **21**, 073033 (2019).

[29] J. Verdú, H. Zoubi, C. Koller, J. Majer, H. Ritsch, and J. Schmiedmayer, Phys. Rev. Lett. **103**, 043603 (2009).

[30] K. Henschel, J. Majer, J. Schmiedmayer, and H. Ritsch, Phys. Rev. A **82**, 033810 (2010).

[31] H. Hattermann, D. Bothner, L. Ley, B. Ferdinand, D. Wiedmaier, L. Sárkány, R. Kleiner, D. Koelle, and J. Fortágh, Nat. Commun. **8**, 2254 (2017).

[32] S. Inouye, A. Chikkatur, D. Stamper-Kurn, J. Stenger, D. Pritchard, and W. Ketterle, Science **285**, 571 (1999).

[33] J. Stenger, S. Inouye, A. P. Chikkatur, D. M. Stamper-Kurn, D. E. Pritchard, and W. Ketterle, Phys. Rev. Lett. **82**, 4569 (1999).

[34] S. Slama, S. Bux, G. Krenz, C. Zimmermann, and P. W. Courteille, Phys. Rev. Lett. **98**, 053603 (2007).

[35] H. Ritsch, P. Domokos, F. Brennecke, and T. Esslinger, Rev. Mod. Phys. **85**, 553 (2013).

[36] S. Ostermann, F. Piazza, and H. Ritsch, Phys. Rev. X **6**, 021026 (2016).

[37] J. A. Muniz, D. Barberena, R. J. Lewis-Swan, D. J. Young, J. R. Cline, A. M. Rey, and J. K. Thompson, Nature (London) **580**, 602 (2020).

[38] H. Keßler, J. G. Cosme, C. Georges, L. Mathey, and A. Hemmerich, New J. Phys. **22**, 085002 (2020).

[39] F. Ferri, R. Rosa-Medina, F. Finger, N. Dogra, M. Soriente, O. Zilberberg, T. Donner, and T. Esslinger, Phys. Rev. X **11**, 041046 (2021).

[40] B. P. Marsh, Y. Guo, R. M. Kroeze, S. Gopalakrishnan, S. Ganguli, J. Keeling, and B. L. Lev, Phys. Rev. X **11**, 021048 (2021).

[41] F. Mivehvar, F. Piazza, T. Donner, and H. Ritsch, Adv. Phys. **70**, 1 (2021).

[42] I. B. Mekhov, C. Maschler, and H. Ritsch, Nat. Phys. **3**, 319 (2007).

[43] I. B. Mekhov and H. Ritsch, Phys. Rev. Lett. **102**, 020403 (2009).

[44] J. Keeling, M. J. Bhaseen, and B. D. Simons, Phys. Rev. Lett. **105**, 043001 (2010).

[45] M. Lewenstein, L. You, J. Cooper, and K. Burnett, Phys. Rev. A **50**, 2207 (1994).

[46] B. E. A. Saleh and M. C. Teich, *Fundamentals of Photonics* (Wiley, Hoboken, NJ, 2019).

[47] P. Domokos, P. Horak, and H. Ritsch, Phys. Rev. A **65**, 033832 (2002).

[48] S. Inouye, R. F. Löw, S. Gupta, T. Pfau, A. Görlitz, T. L. Gustavson, D. E. Pritchard, and W. Ketterle, Phys. Rev. Lett. **85**, 4225 (2000).